Broadband Absorption in the Cavity Resonators with Changed Order

Agata Roszkiewicz
Institute of Fundamental Technological Research, Polish Academy of Sciences,
Adolfa Pawińskiego 5b, 02-106 Warsaw, Poland

Keywords: Broadband Absorption, Enhanced Absorption, Localized Surface Plasmons, Cavity Resonances, Diffraction Gratings.

Abstract: This paper presents an analysis of phenomena leading to high and broadband absorption at a structure combined of three elements: one-dimensional dielectric diffraction grating placed between silver grating and a thick silver substrate. Each element of the dielectric grating consists of media of different dielectric constants but of the same geometrical dimensions. A broad spectrum of high absorption in such a structure is achieved as a result of two issues. First, due to the different excitation conditions the cavity resonances are excited at different wavelengths. Second, the changed order of the resonators leads to further broadening of the absorption band.

1 INTRODUCTION

High and broadband absorption of electromagnetic waves is of interest in many nanophotonic applications. Various kinds of configurations were proposed to obtain near zero reflection and trapping of light in the structure. Control of the reflection and transmission is an important issue especially in photodetectors and solar cells (Ferry et. al., 2010). The total absorption of radiation by a metallic structure has attracted significant interests over the past few years (Liu et. al., 2010, Shchegolkov et. al., 2010, Liu et. al., 2011). Many metallodielectric structures designed as nearly perfect absorbers have been proposed and some promising applications have been discussed.

The near perfect absorption may be achieved with use of localized plasmon resonances (Hu et. al., 2009, Kravets et. al., 2010, Liu et. al., 2011, Pan et. al., 2013), gap plasmons in bottle-like cavities (Meng et. al., 2013), propagating surface plasmon polaritons (Chen et. al., 2010) or Fabry-Perot resonances in cavities between two metal surfaces (Diem et. al., 2009, Hao et. al., 2010, Roszkiewicz et. al., 2012, Song et. al., 2013). The designs based on a Fabry-Perot resonance usually are composed of periodic gratings. In order to obtain a wide absorption band, each period of the structure can be made of resonators of varied dimensions, supporting resonances at different wavelengths (Song et. al., 2013, Koechlin et. al., 2011, Zhang et. al., 2013, Wang et. al., 2013). The continuation of such a structure is a quasiperiodic structure (Dolev et. al., 2011) and chirped grating with slowly varying period (Chen et. al., 2010, Bouillard et. al., 2012, Gan et. al., 2011). In those periodic configurations the wide absorption band is a result of the existence of similar resonances occurring at neighbouring frequencies. However, in those examples all cavities are filled with the same material and the resonators are ordered according to their resonance wavelengths.

In this paper we analyse a one-dimensional (1D) absorptive structure. The presented configuration is based on a 1D dielectric diffraction grating placed between silver grating and a thick silver substrate. The structure realizes simultaneous suppression of reflection and transmission, leading to enhanced absorption. Each element of the dielectric grating consists of dielectric medium of different dielectric constant but of the same geometrical dimensions. A broad spectrum of high absorption in such a structure is achieved as a result of the horizontal cavity modes (HCMs) excited at different wavelengths. Moreover, the changed order of the resonators leads to further broadening of the absorption band. It occurs that the sequence of the resonators influences on the absorption characteristics at normal as well as oblique incidence.

Roszkiewicz A..
Broadband Absorption in the Cavity Resonators with Changed Order.
DOI: 10.5220/0005332900810086
In *Proceedings of the 3rd International Conference on Photonics, Optics and Laser Technology* (PHOTOPTICS-2015), pages 81-86
ISBN: 978-989-758-093-2

2 SIMULATION MODEL AND METHOD

The analysed configuration is depicted in figure 1. A TM polarized plane wave is incident normally from air at a 1D stacked silver and dielectric gratings with subwavelength slits placed at the silver substrate. Each period of the structure consists of $N = 5$ identical metal stripes lying on the dielectric resonators with different dielectric constants. The relative change between dielectric constants of the resonators is denoted by $\Delta\varepsilon$. Hence the dielectric constant of the n^{th} stripe ($n = 1, 2, ..., N$) is $\varepsilon_n = \varepsilon_0 + n\Delta\varepsilon$, where $\varepsilon_0 = 1$ is the dielectric constant of air and $\Delta\varepsilon = 0.8$. We show, that the optimized structure does not consist of resonators placed in order according to the increasing resonance wavelength. The structure characterized by the widest absorption band is the structure, where the sequence of the resonators is: $\varepsilon_5, \varepsilon_2, \varepsilon_4, \varepsilon_1, \varepsilon_3$.

Numerical analysis of the optical response of the structure was performed with use of Rigorous Coupled Wave Analysis with implementation of the scattering matrix algorithm, multilayer extension and the factorization rules. The dielectric function of silver was numerically fitted to the experimental data (Johnson et. al., 1972).

3 SIMULATION RESULTS

It is known that by introducing different resonators in one structure one can obtain a wide absorption spectrum due to the excitation of resonances at different wavelengths. In this paper we utilize the concept of the 1D grating absorber presented in figure 1. The main cause of high absorption in this kind of structure is the excitation of the open metal-dielectric-metal (MIM) horizontal cavity modes in those dielectric resonators. The formation of the cavity mode results in low reflection and strong absorption, making most of electromagnetic field focus inside the cavity. However, usually the resonators are placed in an order accordingly to their resonance wavelengths (Chen et. al., 2010, Song et. al., 2013, Bouillard et. al., 2012). Here we change this order.

Figure 2 gives the calculated absorption as a function of the incident wavelength for configurations with $\Delta\varepsilon = 0.8$ and various orders of dielectric resonators, among others the optimized structure (green dashed line) and the ordered configuration (red dashed-dotted line). The plot

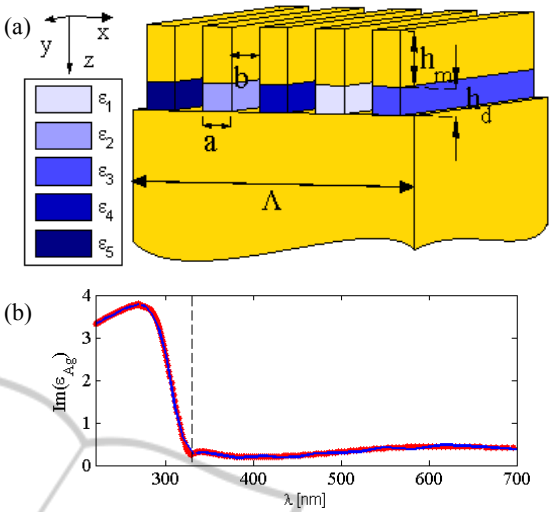

Figure 1: (a) Configuration of the analysed problem. One period of the structure $\Lambda = 380$ nm is presented. Silver 1D grating of thickness $h_m = 25$ nm is placed on the dielectric grating of thickness $h_d = 21$ nm. Dimensions of the equally spaced ridges of identical dimensions: $a = 30.4$ nm, $b = 45.6$ nm and the filling factor $f = 0.4$. (b) Imaginary part of the dielectric function of silver as a function of wavelength. Blue line – experimental data from (Johnson et. al., 1972), red dots – numerical fit. Vertical dashed line denotes $\lambda = 330$ nm.

shows also the absorption curve for different configurations with constant ε_n for comparison (dark grey lines). The absorption spectrum differs for structures with differently arranged resonators, even under normal incidence. Other sequences of the same resonators than the optimized one significantly reduce the absorption bandwidth. It can be seen that the non-optimized configurations are characterized by narrower absorption band than the optimal structure, despite the fact, that all of them consist of the same resonators, however placed in different order. Thus it appears, that the sequence of the dielectric resonators in each grating period is also an important parameter to be optimized. Moreover, the maximal amplitudes of the resonances in structures with constant ε_n are at the level of ~60%, hence they do not assure the high absorption. This behaviour will be discussed later.

Each cavity resonator can be regarded as two single metal-insulator interfaces brought close to each other. In this situation, the dispersion curve of a single interface splits into high and low-energy modes. Here, due to the field symmetry matching, only the low-energy mode is excited. Dispersion curve for the symmetric mode in each cavity depends on its dielectric constant ε and thickness h_d and can be described by the relation:

$$\tanh(k_z h_d/2) = -k_z^{(m)}\varepsilon_n / (k_z \varepsilon^{(m)}) \quad (1)$$

where k_z, ε_n, $k_z^{(m)}$ and $\varepsilon^{(m)}$ are the z-components of the wave vector and the dielectric constants in the dielectric and metal media, respectively (Maier, 2007). A dispersion curve can be drawn for each resonator with the consideration of its thickness and dielectric constant ε_n. Points at this dispersion curve for a given cavity length $a \approx v_h\lambda_p/2$, where $v_h = 1$ denotes the resonance order in the horizontal cavity, allow to obtain the plasmon resonance wavelength for the wave vector $k = 2\pi/\lambda_p = \pi v_h/a$. Hence, the energy in the resonator can be spatially restricted by metal interfaces (in the vertical direction) and by large wave vectors of the supported plasmon modes (in the horizontal direction).

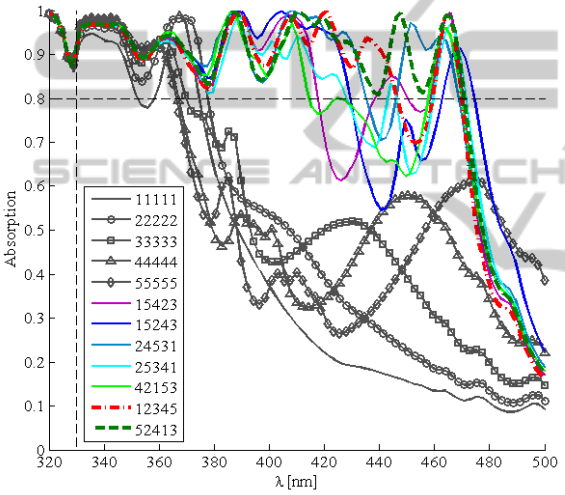

Figure 2: Absorption spectrum as a function of wavelength for exemplary structures with differently ordered resonators under normal incidence. Legend shows configurations of the resonators in each period, green dashed line and red dashed-dotted line show the absorption of the optimized structure and the structure with ordered resonators, respectively. Dark grey lines show the absorption of the structures with all identical resonators within the period. Horizontal dashed line denotes absorption level of *80%*. Vertical dashed line denotes $\lambda = 330$ nm.

The excitation conditions for cavity modes are different in each resonator since, having the same dimensions, the resonators are filled with media of different dielectric constants. This results in frequency splitting of the resonance curves originating from the particular HCMs and thus widening of the total absorption band. In the presented configuration those electric dipole resonances correspond to peaks between *380 – 500* nm wavelength.

High absorption at wavelengths shorter than *330* nm does not originate from any of the plasmonic resonances. The limit value of the wavelength where silver is characterized by low inner loss is about *330* nm. For shorter wavelengths the imaginary part of the dielectric function of silver increases rapidly (figure 1(b)). Hence, high absorption at wavelengths lower than *330* nm visible in presented figures arises from phenomena related to conduction and bound electrons and it is caused by the interband transitions of electrons in metal. For this reason the width of the absorption band is calculated for wavelengths longer than *330* nm. Resonances between *~330-380* nm are connected with the excitation of localized surface plasmons (LSPs), mainly at the metal ridges.

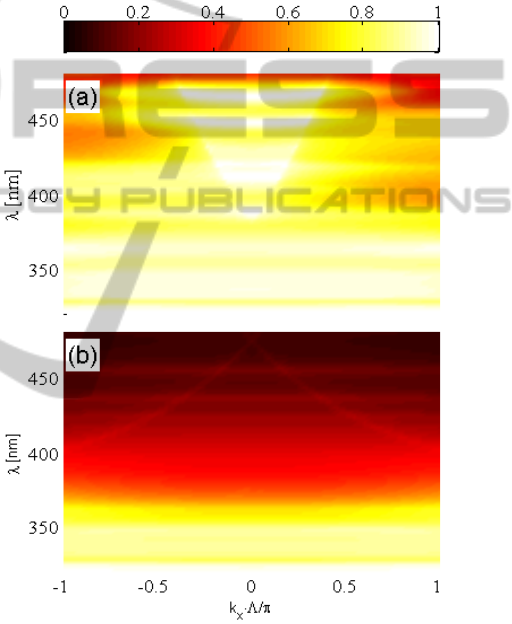

Figure 3: Absorption spectrum as a function of wavelength and incident wave vector for (a) the optimized structure and (b) structure with $\varepsilon_n = \varepsilon_1$.

The width of the band of more than *80%* absorption efficiency at normal incidence for the optimized structure increased of *~121* nm in comparison to the absorption band of the structure with $\varepsilon_n = \varepsilon_1$, where $n = 1, 2,...,5$. Hence, the absorption band width at normal incidence is estimated to be *~141* nm, which can be compared with *~23* nm bandwidth of the $\varepsilon_n = \varepsilon_1$ structure. This gives about *6.1*-fold increase of the stop band width in the optimized structure. Moreover, the bandwidth of the ordered structure is ~116 nm, which gives almost 1.2-fold increase of the absorption bandwidth resulted from the changed order of the resonators.

In order to further analyse the properties of the

modes responsible for high absorption, in figure 3 we present the absorption spectra as a function of wavelength and in-plane component of the incident field wave vector for the optimized structure and the structure with $\varepsilon_n = \varepsilon_1$. First, it is worth to point out that all resonances taking part in enhanced absorption are dispersionless, which excludes excitation of propagating surface plasmon polaritons.

Second, since at $\lambda = \Lambda = 380$ nm the +/- 1^{st} propagating diffraction orders appear, it is of interest to design the structure so that all the HCMs are excited at longer wavelengths, in the zero-order regime, as presented. This prevents from unwanted loss of energy which, otherwise, is distributed between the propagating orders and may cause lowering of the HCMs excitation efficiency.

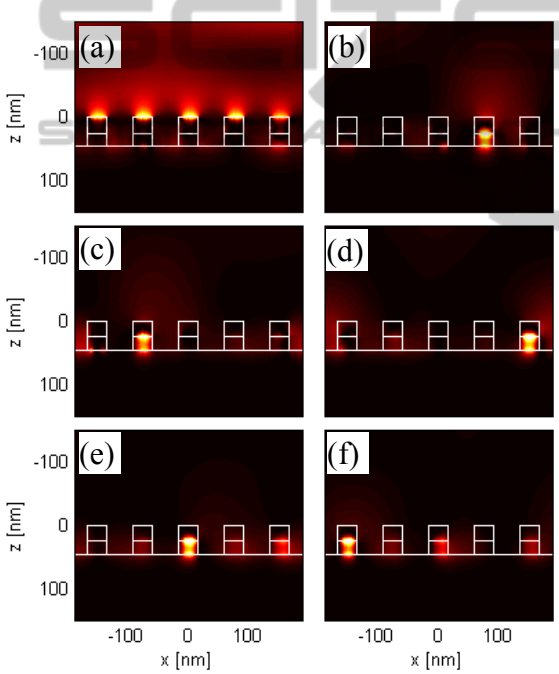

Figure 4: Magnetic field intensity distribution under normal incidence in one grating period of the optimized structure at the peak wavelengths: *364*, *387*, *411*, *428*, *447* and *465* nm. Colour maps at each plot are scaled independently.

Third, whilst the LSP resonances at wavelengths *330-380* nm do not exhibit any dependence on the incidence angle sign, resonances at longer wavelengths show this dependence. The asymmetry in absorption is clearly visible at wavelength range corresponding to the cavity modes. The absorption remains very high for the illumination in the zero-order regime, but outside it lowers and shows an asymmetry withe regard to the incidence angle sign. This indicates the energy losses by the existence of the propagating orders and the coupling between HCMs in neighbouring resonators, which therefore are not independent from each other. Similar asymmetry occurs also for structures with other sequences of resonators.

In order to confirm the physical origin of the suppressed reflection, in figure 4 we investigate the magnetic field distribution at the peak wavelengths under normal incidence. There is a distinct property shown in those plots. Besides the LSP at shorter wavelengths (figure 4(a)), the excitation of HCMs in subsequent resonators is presented (figures 4(b-f)). The sequence of the excited resonances corresponds to the increased dielectric constant. Accordingly to the standing wave model, the plasmon cavity mode excited in each resonator at the upper and lower metal/dielectric surface is reflected from both open ends in a way that the magnetic field shows minima at the ends. This feature is observed in the presented magnetic field distribution plots.

4 DISCUSSION

In this paper, for simplicity, the relative change between dielectric constants in dielectric resonators is assumed constant ($\Delta\varepsilon$) and the dimensions of all of the resonators are equal. However, since slits of the nanometric thickness can be regarded as media with a large refractive index (Astilean et. al., 2000), manipulation of the dielectric grating thickness can also significantly change the resonance wavelength. Accordingly to the simple standing wave model, decrease of h_d results in the decrease of the resonance wavelength and increase of the separation between HCMs absorption peaks. It is worth to point out that when very narrow resonators are considered (h_d of order of few nm), the nonlinear effects may become important (Moreau et. al., 2013). Similar results origin from increasing $\Delta\varepsilon$. Hence, the dielectric constants and thickness of the subsequent resonators can be adjusted to create a desired absorption bandwidth, since both parameters influence the value of the cavity plasmon wave vector.

The physical mechanism of the significant fluctuations in absorption band caused by changed order of the resonators is the mismatch of the phase between individual resonators. It means that the resonators are not independent and are close enough to each other to influence their resonance conditions. The optimized phase related to the spaces between chirped resonators leads to wide and high absorption

band (Song et. al., 2013). Additionally, the mutual influence of the resonators is confirmed, when we analyse the structures with constant ε_n. This is because the peak absorption in those structures is about ~60%. However, the phase change introduced by the change of ε_n in neighbouring resonators alters the resonance conditions in each resonator and leads both to shift of the absorption peaks and high and broadband absorption.

The ordered structure (with resonators in order: ε_1, ε_2, ε_3, ε_4, ε_5), similarly as used in (Song et. al., 2013), may not necessarily be the one with the widest band width. Probably for this reason, in (Song et. al., 2013) further optimization of the structure (individually assorted widths and distances between particular resonators) was performed to achieve broad absorption band. This confirms that the resonators are not independent on each other and the resulted coupling modes play a role in forming the broad absorption band. This indicated also, that the further optimization of our structure by adjusting separately widths of each space between resonators may be possible.

5 CONCLUSIONS

A wide-band absorption over *80%* was obtained in the visible range in the periodic metallodielectric structure with resonators filled with dielectrics of varied dielectric constants. It occurred that this device is sensitive to the change of the resonators' order. The extended broadband absorption in such a grating structure was attributed to the changed sequence of those resonators in comparison to the ordered structure. Those differences indicate that those resonator are not independent on each other. Change of the resonators' order allow for lowering the mismatch of the phase between individual resonators. The width of the absorption band at normal incidence is estimated to be *~141* nm, which is about *6.1* times wider than for a structure with five identical resonators of $\varepsilon_n = \varepsilon_1$. Moreover, the bandwidth of the optimized structure shows almost 1.2-fold increase with respect to the absorption bandwidth of the ordered structure. This work shows a way to obtain a wideband absorption by optimizing order of the different resonators in a grating period. The presented results may appear useful in detection and imaging at visible frequencies, angle-selective absorbers, microbolometers, photodetectors and solar cell technology.

REFERENCES

Astilean, S., Lalanne, P., Palamaru, M., 2000. Light transmission through metallic channels much smaller than the wavelength, *Opt. Commun.* 175 265.

Bouillard, J.-S., Vilain, S., Dickson, W., Wurtz, G. A., Zayats, A. V., 2012. Broadband and broadangle SPP antennas based on plasmonic crystals with linear chirp, *Scientific Reports* 2 829, 1.

Chen, L., Wang, G. P., Gan, Q., Bartoli, F. J., 2010. Rainbow trapping and releasing by chirped plasmonic waveguides at visible frequencies, *Appl. Phys. Lett.* 97 153115.

Diem, M., Koschny, T., Soukoulis, C. M., 2009. Wide-angle perfect absorber/thermal emitter in the terahertz regime, *Phys. Rev. B* 79 033101.

Dolev, I., Volodarsky, M., Porat, G., Arie, A., 2011. Multiple coupling of surface plasmons in quasiperiodic gratings, *Opt. Lett.* 36 1584.

Ferry, V. E., Munday, J. N., Atwater, H. A., 2010. Design considerations for plasmonic photovoltaics, *Adv. Mater.* 22 4794.

Gan, Q., Bartoli, F. J., 2011. Surface dispersion engineering of planar plasmonic chirped grating for complete visible rainbow trapping, *Appl. Phys. Lett.* 98 251103.

Hao, J., Wang, J., Liu, X., Padilla, W. J., Zhou, L., Qiu, M., 2010. High performance optical absorber based on a plasmonic metamaterial, *Appl. Phys. Lett.* 96 251104.

Hu, C., Liu, L., Zhao, Z., Chen, X., Luo, X., 2009. Mixed plasmons coupling for expanding the bandwidth of near-perfect absorption at visible frequencies, *Opt. Express* 17 16745.

Johnson, P. B., Christy, R. W., 1972. Optical constants of the noble metals, *Phys. Rev. B* 6 4370.

Koechlin, C., Bouchon, P., Pardo, F., Jaeck, J., Lafosse, X., Pelouard, J.-L., Haidar, R., 2011. Total routing and absorption of photons in dual color plasmonic antennas, *Appl. Phys. Lett.* 99 241104.

Kravets, V. G., Neubeck, S., Grigorenko, A. N., 2010. Plasmonic blackbody: strong absorption of light by metal nanoparticles embedded in a dielectric matrix, *Phys. Rev. B* 81 165401.

Liu, X., Starr, T., Starr, A. F., Padilla, W. J., 2010. Infrared spatial and frequency selective metamaterial with near-unity absorbance, *Phys. Rev. Lett.* 104 207403.

Liu, X., Tyler, T., Starr, T., Starr, A. F., Jokerst, N. M., Padilla, W. J., 2011. Taming the blackbody with infrared metamaterials as selective thermal emitters, *Phys. Rev. Lett.* 107 045901.

Maier, S. A., 2007. *Plasmonics: Fundamentals and Applications*, New York: Springer.

Meng, L., Zhao, D., Li, Q., Qiu, M., 2013. Polarization-sensitive perfect absorbers at near-infrared wavelengths, *Opt. Express* 21 A111.

Moreau, A., Ciracì, C., Smith, D. R., 2013. Impact of nonlocal response on metallodielectric multilayers and optical patch antennas, *Phys. Rev. B* 87 045401.

Pan, Z., Guo, J., 2013. Enhanced optical absorption and electric field resonance in diabolo metal bar optical antennas, *Opt. Express* 21 32491.

Roszkiewicz, A., Nasalski, W., 2012. Reflection suppression and absorption enhancement of optical field at thin metal gratings with narrow slits, *Opt. Lett.* 37 3759.

Shchegolkov, D. Y., Azad, A. K., O'Hara, J. F., Simakov, E. I., 2010. Perfect subwavelength fishnetlike metamaterial-based film terahertz absorbers, *Phys. Rev. B* 82 205117.

Song, Y., Wang, C., Lou, Y., Cao, B., Li, X., 2013. Near-perfect absorber with ultrawide band width in infrared region using a periodically chirped structure, *Opt. Commun.* 305 212.

Wang, H., Wang, L., 2013. Perfect selective metamaterial solar absorbers, *Opt. Express* 21 A1078.

Zhang, F., Yang, L., Jin, Y., He, S., 2013. Turn a highly-reflective metal into an omnidirectional broadband absorber by coating a purely-dielectric thin layer of grating, *Prog. Electromagn. Res.* 134 95.